PHOTOGRAPHS OF SOME EFFECTS ON RAIN DROPS OF SHOCK WAVES PRODUCED BY 60-CALIBER AND 20-MM PROJECTILES

F. G. P. Seidl

BOEING AIRPLANE COMPANY

I. Abstract

Projectiles from a 60-caliber and a 20-mm gun were fired through simulated rain drops of diameters 1.7 ± 0.3mm. The projectile velocities were varied from 1900 ft/sec to 4060 ft/sec and in certain cases the intensities of the bow shock waves could be estimated. Motion-picture sequences of the interactions of the projectiles and rain drops were taken by a Fastax high-speed camera setup. Times between successive photographs were approximately 150 microseconds. The impacts of the low shock waves were seen to jar and distort the rain drops which always broke up some 600 to 4000 microseconds later. The times required for breakup seemed to depend upon the shock wave intensity. In cases requiring times of the order of 4000 microseconds, blasts of debris and gaseous explosion products from the gun muzzle may have contributed to the breakup.

II. Introduction

While evaluating the problem of the rain erosion of radomes and leading edges of a supersonic aircraft, the following question arose: What happens to a typical rain drop when struck by the bow shock wave generated by the nose of a supersonic aircraft or by a prong extending out ahead of the nose? The experiment described herein was designed in an attempt to answer this question.

III. Experimental Method

A simple expedience for examining the effects of shock waves on rain drops was to photograph progressively the motion of a projectile and its associated shock waves through simulated rain. The production of rain drops of any desired size was merely a matter of choosing a proper orifice from which water could fall. The intensity of the bow shock waves could be controlled by varying the speed of the projectile and the shape of its nose. A high-speed Fastax motion-picture camera (see Reference 1) was available for photographing the rain drops before and after impact with a bow shock wave. Unfortunately, the camera was not sufficiently fast to stop the motion of the projectiles and to define the shock fronts; although the presence of these can be recognized by their blurred images.

The projectiles were fired from either a 60-caliber or 20-mm gun through the rain drops into a revetment (see Figure 1). For measuring projectile speeds two screens were situated some 8 ft beyond the proint of intersection of the rain-drop stream and the line of fire. Each screen was a one-foot square wooden frame strung with fine copper wires which had to be replaced after each shot. The time required for each projectile to traverse the distance between the successive screens was measured by a crystal-controlled chronometer.

The optical system (see Figure 2) consisted of the following elements mounted in a line: (1) A zirconium low-voltage arc light (Sylvania C-100) located 60 inches from a first collimating lens, (2) A pair of 6-inch diameter converging lenses mounted 30 inches apart and (3) A 16-mm Fastax high-speed camera (see Reference 1) situated 60 inches from the second lens. The arc was at the focus of the first lens which formed a region of collimated light. The second lens collected this light and focused it on the camera's iris diaphragm which was set at f/22. The rain fell through the region of collimated light between the two lenses. Both the drops and the projectiles appeared on the photographs as shadows. Actually, the drops were dark because they refracted light out of the camera. On the other hand, the projectiles formed true shadows by intercepting the light. Moreover, the photographed sizes of the rain drops and the projectiles were independent of their distances from the camera.

The Fastax camera (see Reference 1) exposed a continuously moving film. The shutter action was produced by a high-speed rotating parallel-sided prism. The latter was synchronized by gears with the moving film. Electric power for operating the camera was obtained from a booster circuit (see References 1 and 2). In order to gain a rapid acceleration of both the rotating prism and the film reels, the booster circuit supplied power at 300 volts for the first 100 milliseconds of operation, at 290 volts during the second 100 milliseconds and at 280 volts for the remainder of a run. In typical operation only the final 20 feet of a 100-foot reel of film was moving at the maximum speed of 8000 frames per second. The exposure time was equal to the reciprocal of the product of the number of frames per second and 5.6. The firing of the gun was always delayed 0.6 seconds after starting the camera in order to allow it to approach full speed. Finally, Super XX 16-mm film or its equivalent was used in all runs.

The artificial rain drops were produced by the breakup of a fine stream of water emerging from a single 0.035-inch hole drilled at the end of a pipe which was joined to a 50-gallon drum. The latter was supported so that the 0.035-inch hole was 10 feet directly above the point of intersection of the line of fire and the optical axis of the camera. In falling the stream broke up into cigar-shaped slugs of water, each of which formed into a spherical drop. This fact and the relation between droplet diameter and orifice diameter has been explained by Lord Rayleigh (see Reference 3).

The water stream and droplets fell through a 4-inch tube which acted as a wind shield. The simulated rain appeared on the photographs as spherical drops about 1.7 ± 0.3 mm in diameter (see Table I). An indication of the horizontal and vertical separations between drops can be seen in the photographs. Usually, the drops landed within a horizontal circle of 2-inch diameter. By running the film through a motion-picture projector, the larger drops were seen to fall faster than the smaller ones, as was expected.

Three types of projectiles were used; see Figure 3. Two of the three types were fired in an unrifled 60-caliber gun. The lack of spin permitted these projectiles to tumble; however, as may be seen from the photographs, when the projectile was traversing the rain, the tumbling had not yet become appreciable. Of the 60-caliber projectiles, one type was a right circular cylinder of diameter 0.599 inches and of one-inch length, the other type had a conical nose of 60° full apex angle. The 60-degree cone was chosen because data were available on the shock fronts produced by such projectiles. The third type of projectile was from a standard 20-mm shell. The 20-mm projectiles were rifled but this did not seem to modify appreciably their bow shock waves; for photographs of 2-pound spinning projectiles in motion see Reference 4.

IV. Experimental Procedure

Each firing of a projectile through simulated rain was carried out according to the following program:

(1) The Fastax camera was loaded with 100 feet of Super XX 16-mm film.

(2) The bearings of the rotating parts of the camera were lubricated with special oil.

(3) The light source and the chronograph were turned on.

(4) The simulated rain was allowed to fall.

(5) The camera was started simultaneously with a time-delay device, which some 0.6 seconds later, fired the gun.

(6) The reading of the chronometer was recorded and this was the time required for the projectile to traverse the ten feet between the wooden screens.

V. Results

Twenty-one motion-picture sequences were obtained each showing the effects of firing a projectile through simulated rain. Of these, ten were taken of 60-caliber conical-nose projectiles whose speeds ranged from 2460 ft/sec to 4060 ft/sec. Six of the shots were with 20-mm projectiles which travelled at 2660 ± 40 ft/sec. Five shots were made using bluff cylindrical 60-caliber cylinders travelling about 1900 ± 100 ft/sec; chronologically, these were the first shots fired, but they are mentioned last becuase their speed measurements were unsatisfactory. Finally, one sequence was taken of a conical-nose projectile fired without any rain. Because of an improved setup, there was less horizontal spreading of the rain drops in the shots using the conical-nose projectiles and the 20-mm ammunition.

All projectiles were fired at supersonic speeds and any rain drop not having experienced a direct impact with a projectile was subject to a series of effects as follows:

(1) Impact of the bow shock wave that originated from the region near the nose of the supersonic projectile.

(2) The Prandtl-Meyer expansion waves that arose mainly from the shoulder region of the projectile.

(3) Impacts from secondary shock waves which originated from the rear of the projectile and from its turbulent wake.

(4) The debris and gases from the propelling explosion came last.

The strength of the bow shock wave can be estimated for the conical-nose projectiles (see Table II). The other effects were relatively weak except for the debris and gases from the propelling blast. The place of entry of this last effect could be seen in the photographs under consideration.

The results which were evident from the motion-picture sequences are given below:

(1) Nowhere was there evidence that rain drops were immediately broken up by the impacts of the bow shock waves. Apparently there were several cases where, through a direct hit with a projectile, rain drops were instantly broken up into a fine spray. Dark smudges or dark clouds in certain pictures can be explained as due to the refraction effects of a great many tiny liquid droplets and not by regions of high water vapor content or of possible air-density changes (see Section VI, C).

(2) The rain drops were jarred and immediately deformed by a bow shock wave. In many instances the drops broke up before the blast of debris and gases from the gun muzzle swept by. The time required for drop breakup depended upon the strength of the shock wave, but was never less than about 600 microseconds (μsec). Drops further away from the line of fire took longer to break up. Those drops which were situated closest to the line of fire of the bluff-nose cylindrical projectiles broke up first (e.g., 600 μsec in shot 19); here each of the bluff-nose projectiles produced a strong local bow shock which may have been stronger in the vicinity of the nose than for other types of projectiles, but whose intensity certainly fell off more rapidly with distance from the line of fire.

(3) It was found that the exposure times were 20 to 27 μsec and the times between successive frames were 115 to 160 μsec. The exposure times and the inter-frame periods were calculated from (a) Blurs in the images of projectiles and their associated shock fronts, and (b) The change in projectile positions between successive frames. The operation of the camera was such that the inter-frame period was equal to 5.6 times the exposure time.

TABLE I CHARACTERISTICS OF NATURALLY OCCURRING PRECIPITATION*

(Air Density as at 0°C and 740 mm Press.)

Popular Name	Precipitation Intensity mm/hr	in/hr	Droplet Diam. mm	Velocity of Fall Rates Meters per sec.	Milligrams of liquid water per cu meter of air	Grains of Liquid Water per cu ft of air
Clear	0.00	--	--	--	0.00	--
Fog	Trace	--	-.01	0.003	6.0	0.002
Mist	0.05	0.002	0.10	0.25	55.5	0.024
Drizzle	0.25	0.01	0.20	0.75	92.6	0.04
Light Rain	1.00	0.04	0.45	2.00	138.9	0.06
Moderate Rain	4.00	0.16	1.0	4.00	277.8	0.12
Heavy Rain	15.00	0.59	1.5	5.00	833.3	0.365
Excessive Rain	40.0	1.6	2.1	6.00	1851.9	0.81
Clous-burst	100 to 1000	4.0 to 40.0	3.0	7.00	4000 to 35000	1.75 to 15.30

* F. A. Berry, Jr., E. Bollay and N. R. Beers, Handbook of Meteorology, McGraw Hill (1945).

TABLE II SHOCK-FRONT ANGLES AND PRESSURE STEPS IN THE CASE OF 60-DEGREE APEX ANGLE CONES FIRED AT VARIOUS SPEEDS

Shot Number	Projectile Speed	Mach Number	Angle between conical part of bow shock front & line of fire*	Pressure ratio across the true conical part of the shock front**
	ft/sec	M	Degrees	P_1/P_o
1	4060	3.64	38.0	5.63
2	3690	3.29	38.8	4.76
3	3140	2.80	41.3	3.80
4	2910	2.60	42.3	3.42
6	2730	2.44	43.3	3.14
8	2510	2.24	45.5	2.78

* Cf. Fig. 11, p. 467, J. W. Maccoll, Proc. Roy. Soc. A, vol. 159, p. 459 (April 1937).

**Interpolated from the results of Table II, p. 285, G. I. Taylor and J. W. Maccoll, Proc. Roy. Soc. A, vol. 139, p. 278 (Feb. 1933).

(4) Not later than 2500 to 4000 μsec after the passage of a projectile, the rain drops always had broken up if initially they were within about 2 1/2 inches of the line of fire at the moment of firing. The ultimate breakup times were clustered about 2500 μsec in the cases of 20-mm shots and were nearer to 4000 μsec for 60-caliber conical-nose projectiles. However, before the elapse of 4000 μsec the drops had been overtaken by the blast of gaseous explosion products and there was some question as to the contribution of the latter to the breakup.

VI. Discussion

A. Shock Waves Produced by the Projectiles

The three types of projectiles were fired at supersonic speeds and any projectile travelling through air faster than the speed of sound produces a bow shock wave (see Reference 5). The surface of this shock wave is approximately conical and symmetric relative to the line of fire. The apex of the cone lies near the nose of the projectile and may be either just a little ahead of the nose or attached to it depending upon both the shape of the latter and the ratio of projectile speed to the speed of sound. The forward-most portion of the shock wave is its apex; from here the shock front bends back away from the direction of motion. In fact, the faster the projectile is moving, the more acutely its shock front bends back.

The shock wave separates one region of constant pressure, P_0, density and air velocity lying ahead of it from another region of relatively constant pressure, P_1, density and air velocity lying behind. In the cases which concern the projectiles fired against rain, the thicknesses of the transition regions were of the order of 10^{-3} to 10^{-4} mm (see References 6 and 7); i.e., the shock-wave thicknesses were much less than the diameters of naturally occurring rain drops (see Table I).

Of the three types of projectiles, the bluff-nose cylindrical ones produced bow shock waves which were the most intense (i.e., P_1/P_0 was largest) in regions very close to the nose; but in these cases the intensities fell off more rapidly with distance away from the line of fire (see Reference 8). On the other hand, most was known about the intensities of the shock waves produced by the conical-nose projectiles; values are given in Table II for both the pressure change across a bow shock front and its inclination as a function of projectile speed. These values are good for regions near the nose and had been obtained theoretically and had been checked by measurements (see References 9 and 10). Finally, the 20-mm projectiles were available for firing and offered a variation of type of bow shock which might be more comparable to that formed by the nose of a supersonic aircraft.

In the case of actual projectiles (see References 8 and 11), the pressure ratio P_1/P_0 always tends to fall off with increasing distance from the flow axis (i.e., the line of fire). In particular, it was found that (see Reference 11), for a 60° conical-nose projectile, the pressure ratio P_1/P_0 falls to roughly 0.7 of the values given in Table II at a point distant some 4R from the flow axis; R denotes the cross-sectional radius of the projectile. A decrease in slope of the shock front relative to the direction of motion is another manifestation of the decrease in shock intensity with increased distance away from the flow axis. In the case of a full 60° conical-nose projectile, the decrease in shock slope is gradual and does not become very appreciable at regions closer than 4R to the flow axis (see References 9 and 11).

Shadow photographs of projectiles and their shock waves have been taken by the Ballistic Research Laboratory, Aberdeen, Md. One such photograph shows the shock waves produced by a 155-mm projectile travelling at a speed of Mach 2.479 (see Reference 12) and very little decrease in the slope of the bow shock front is evident out to 8R. However, this photograph is not directly applicable to those projectiles which were fired through the rain drops becuase it shows a more "streamlined" projectile and the nature of flow around a supersonic projectile is such that any abrupt changes in shape create secondary effects which cause the bow shock wave to fall off more rapidly.

B. Period of Small Surface-Tension Oscillations

The theory of small surface-tension oscillations of a liquid drop about a spherical form has been worked out by Lord Rayleigh (see Reference 13). The shape of the surface of the oscillating drop can be expressed as a superposition of several harmonically time-dependent deformations each characterized by a particular Legendre polynomial. The most important mode of oscillation occurs for the Legendre polynomial of order $n = 2$; this means that the drop configuration oscillates between a dumbbell shape and a flattened sphere, where the flattened regions are slightly concave. Values of the period of oscillation for $n = 2$ are set out in Table III.

TABLE III SMALL SURFACE-TENSION OSCILLATIONS

Diameter of Water Drop (mm)	Period of Oscillation T (μsec)
1.0	2900
1.5	5300
2.0	8200

It is interesting to note that the observed times between a typical impact of a bow shock wave with a rain drop and drop breakup are of the same magnitudes as the time required by a small surface-oscillation to change a sphere into either the slightly dumbbell-type configuration or into a flattened sphere; i.e., for water drops whose sizes are the same as in the simulated rain, (1/4)T equals 1000 μsec to 4000 μsec. Moreover, in certain motion-picture sequences rain drops having been struck by a bow shock wave appeared to grow into flattened spheres and ultimately into a sort of doughnut-shaped objects before breaking up.

In at least one case (see shot No. 20), a drop of rain having absorbed energy from the impact of a shock wave changed into a dumbbell shape before breaking up. However, since the theory of surface-tension oscillations only applies to small oscillations, it cannot be concluded without further consideration that the shock-wave impacts excited surface oscillations in the rain drops and that these oscillations were of sufficient amplitudes to break up the drops.

The time of transit of a compression wave through the body of a typical rain drop should have been

$$(1.7 \text{ mm})/v = 1.2 \ \mu\text{sec},$$

where v denotes the velocity of sound in liquid water (v = 4750 ft/sec). The fact that the drop breakup times were some thousands of times greater than 1.2 μsec is further evidence that the breakup mechanism is related to a surface effect.

C. Interpretation of Dark Clouds on Some Pictures

In certain photographs a dark cloud suddenly appeared and slowly dissipated. Such clouds always formed adjacent to the blurred image of a projectile and in a region which previously had contained a rain drop. In all cases it was possible to associate the formation of one of these clouds with a direct impact of a projectile and a rain drop. However, the transformation of a rain drop of 1.7-mm diameter into a cloud some hundreds of times larger in area was surprising and, consequently, some explanation was sought.

Suppose that in the optical setup depicted in Figure 2, there was a local anomaly in the refractive index throughout some region of the order of a cubic inch in size and which was located somewhere between the two collimating lenses. Let the anomalous refractive index be denoted by $n + \Delta n$ compared to an index equal to n everywhere else. Light which passed in and out of the anomalous region would be refracted so that it no longer would be brought to a focus at the center of the iris diaphragm of the camera. According to the laws of refraction, it can be shown that the light which passed through the anomalous region would be focused on a point that is at a distance δ from the optical axis of the camera. The magnitude of δ is given by the following relation:

$$\delta(\text{inches}) = 60\,\epsilon;$$
$$\epsilon \cong (\Delta n/n) \tan \phi;$$

here ϕ denotes the angle between the incident ray and a normal to the surface of the anomalous region. If the diameter of the camera aperture were 0.1 inches, then a value of Δn equal to or greater than $(0.05/60) \cot \phi = 0.000833 \cot \phi$ would be necessary to reflect light out of the camera.

The difference between the refractive index of water and air is 0.333. Since this is the equivalent Δn for a rain drop, the latter would refract light out of the camera for all angles of incidence down to $\phi = \text{arc cot } (0.333/0.000833) = 0.1°$ and this effect must have been responsible for making the rain drops appear as little dark circles.

On the other hand, water vapor has a refractive index of 1.00025 compared to n = 1.00029 for air. In order for water vapor to refract light out of the camera, the following relation must be satisfied:

$$60 \times (1.00029 - 1.00025) \tan \phi \gtrsim 0.05 \text{ inches}$$

or

$$87^\circ \lesssim \phi < 90^\circ.$$

Physically this means that, even if a region were to be 100% water, only a portion of its periphery corresponding to $87^\circ \lesssim \phi < 90^\circ$ would be able to refract light out of the camera.

Thus, the dark clouds which appeared on certain photographs must be due to sizeable variations in refractive index such as can be attributed to liquid water itself. Consequently, these clouds are indications that a rain drop is atomized into liquid spray by impact with a supersonic projectile.

VII. Acknowledgment

The cooperation of the following persons is gratefully acknowledged. The Fastax camera equipment was supplied and set up by George Hays of the Boeing Airplane Company Power Plant Unit. During most of the runs the camera was operated by either W. Tribou or H. Tacker. The guns were set up and fired under the direction of Andy Dussik, Bomber Weapons Unit.

REFERENCES

(1) Bulletin on Fastax High-Speed Motion Picture Cameras, Wollensak Optical Co., Rochester 21, New York.

(2) Model J-410 Fastax Control Unit ("The Goose"); Instruction Book No. 1262, Industrial Timer Corporation (Oct. 15, 1948).

(3) J. W. Strutt (Lord Rayleigh), Theory of Sound, Dover (1945) vol. II, p. 362.

(4) J. W. Maccoll, Proc. Roy. Soc. A, Vol. 159, p. 459 (April 1, 1937).

(5) R. Courant and K. O. Friedricks, Supersonic Flow and Shock Waves, Interscience (1948).

(6) H. W. Liepmann, A. Roshko and S. Dhawan, On Reflection of Shock Waves from Boundary Layers, NACA Report 1100 (1952).

(7) A. E. Puckett and H. J. Stewart, Quar. of Appl. Math., vol. VII, p. 457 (Jan. 1950).

(8) J. H. Giese and V. E. Bergdolt, Jour. of Appl. Phys., vol. 24, p. 1389 (Nov. 1953).

(9) G. I. Taylor and J. W. Maccoll, Proc. Roy. Soc. A, vol. 139, p. 278 (Feb. 1933).

(10) J. W. Maccoll, Proc. Roy. Soc. A, vol. 159, p. 459 (April 1937).

(11) F. D. Bennett, W. C. Carter and V. E. Bergdolt, Jour. Appl. Phys., vol. 23, p. 453 (April 1952).

(12) T. von Karman, Jour. of the Aeronaut. Scies., vol. 14, p. 373 (July 1947)..

(13) See page 373 of Reference (3) or H. Lamb, Hydrodynamics, Dover (1945), p. 475.

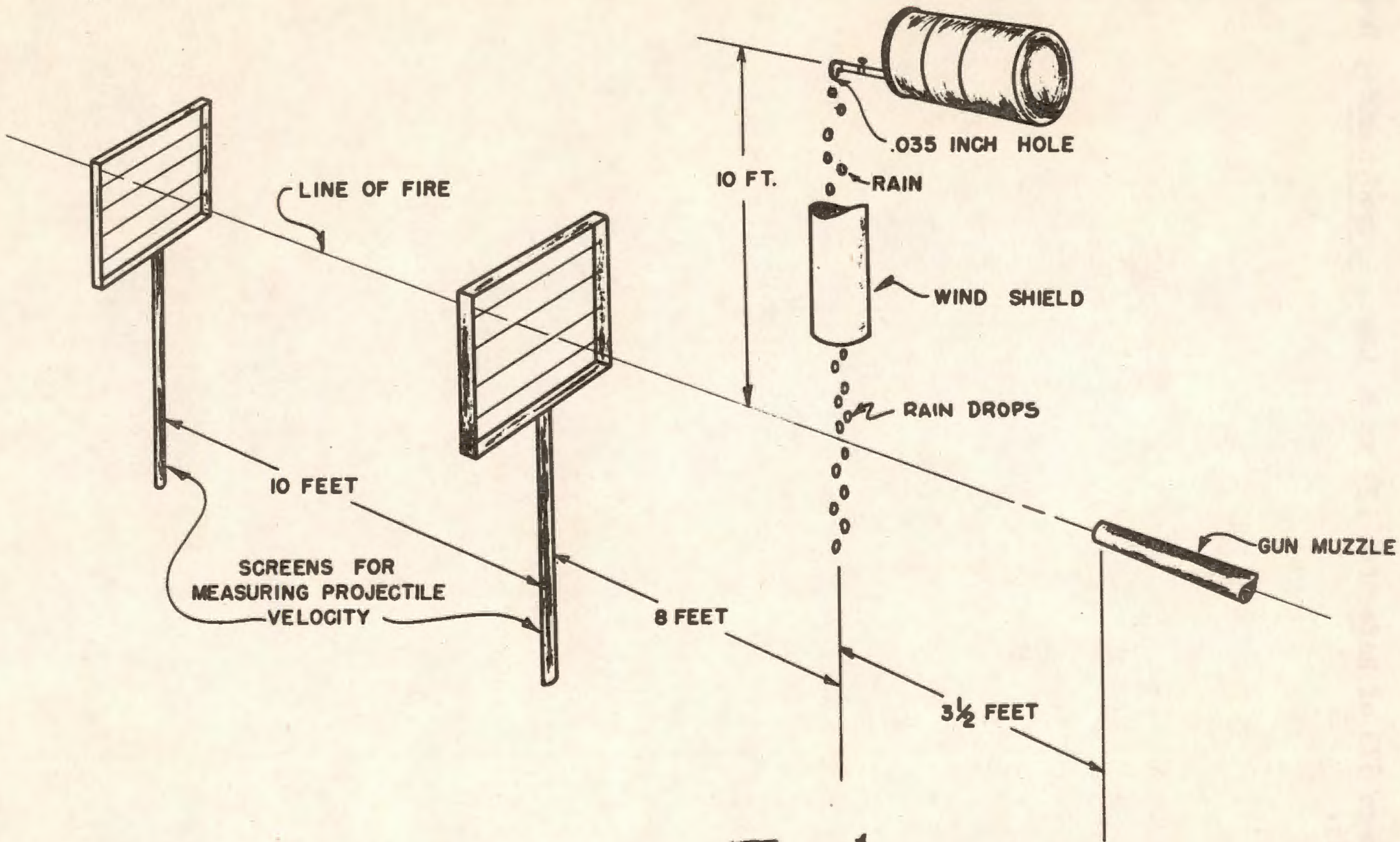

Fig. 1

ARRANGEMENT FOR STUDYING EFFECTS OF PROJECTILE SHOCK WAVES ON RAIN DROPS

(VIEW ALONG LINE OF FIRE)

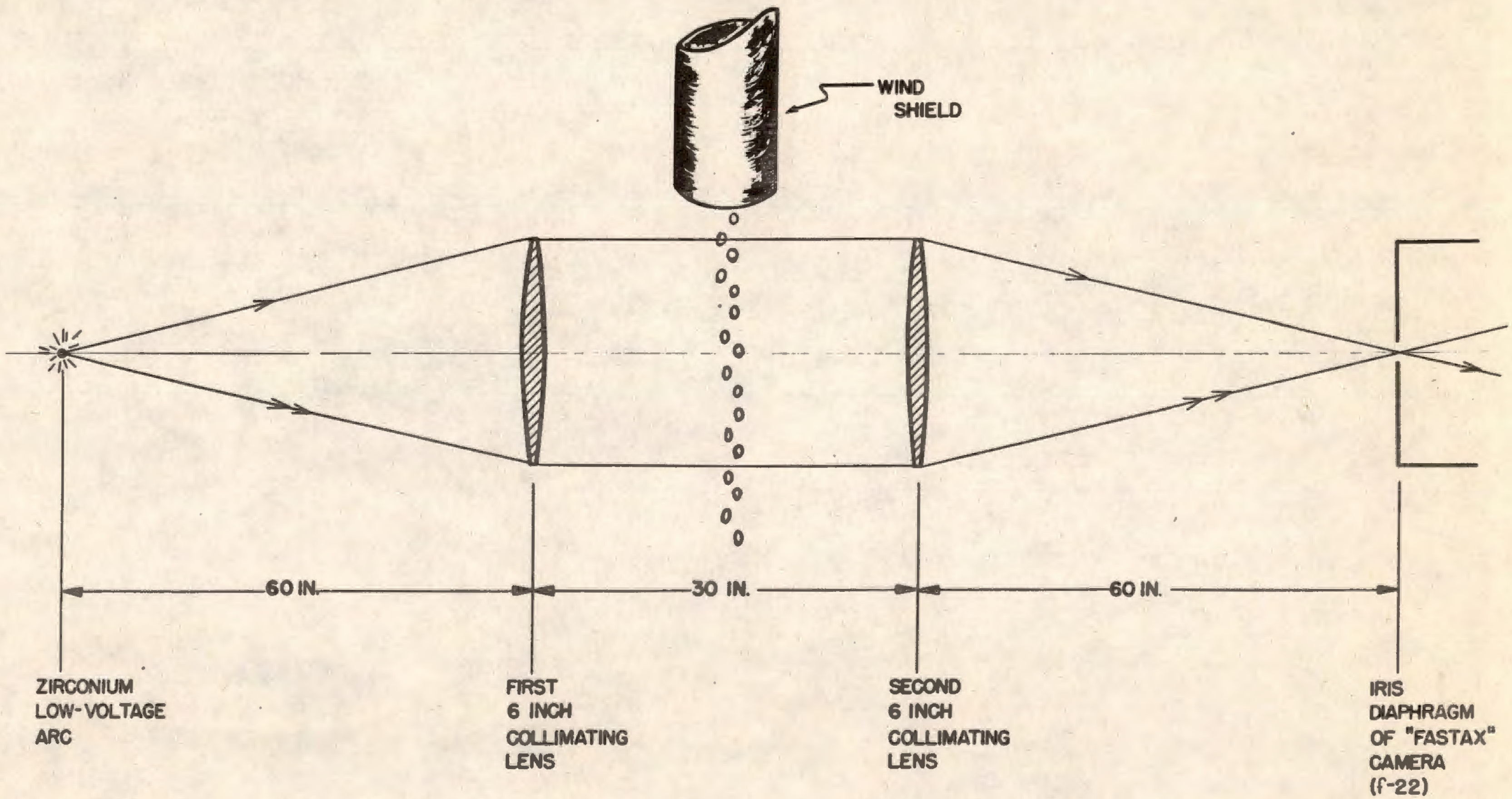

FIG. 2

ARRANGEMENT FOR STUDYING EFFECTS OF PROJECTILE SHOCK WAVES ON RAIN DROPS

(VIEW ALONG AXIS OF CAMERA)

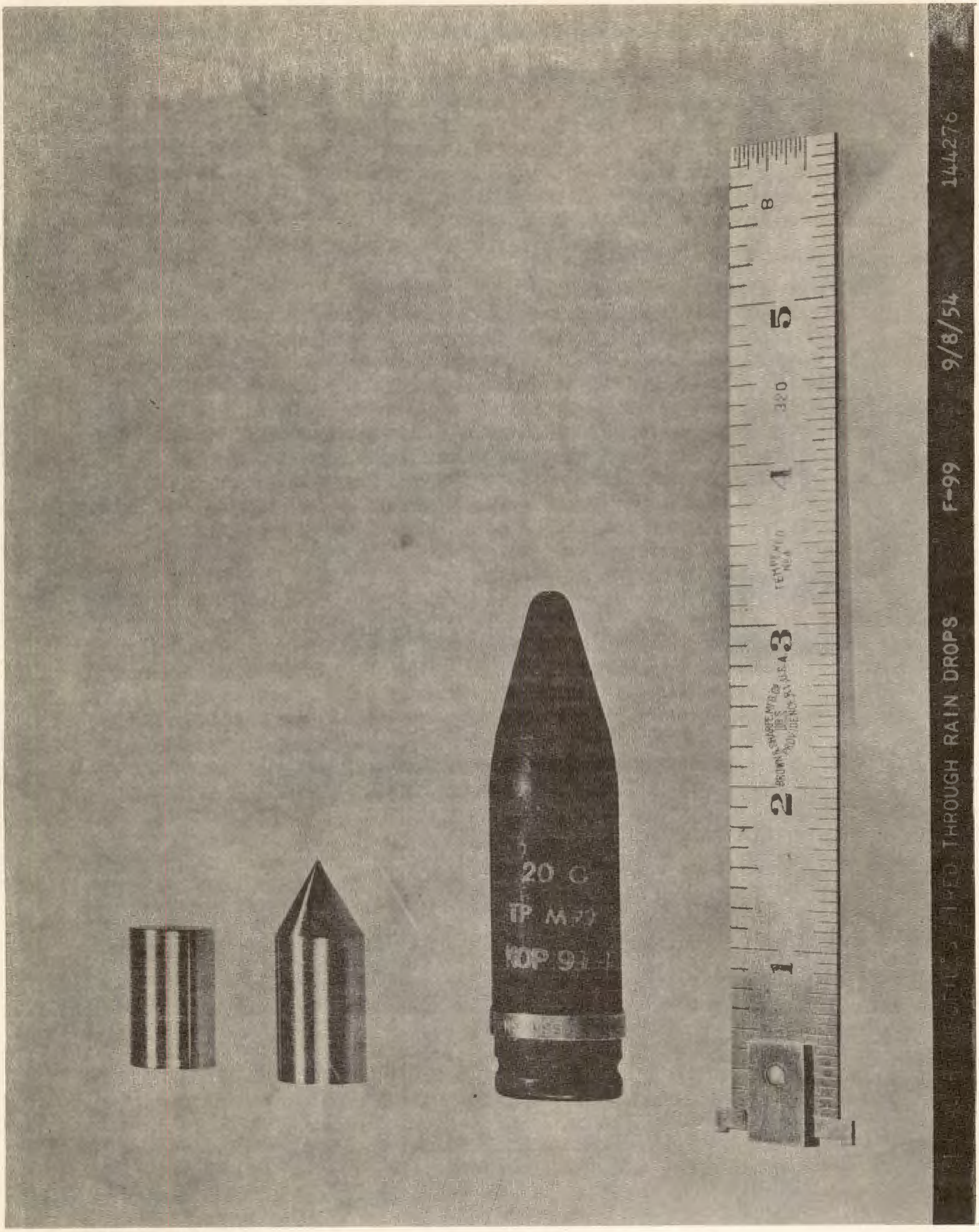
THROUGH RAIN DROPS
F-99
9/8/54
144276

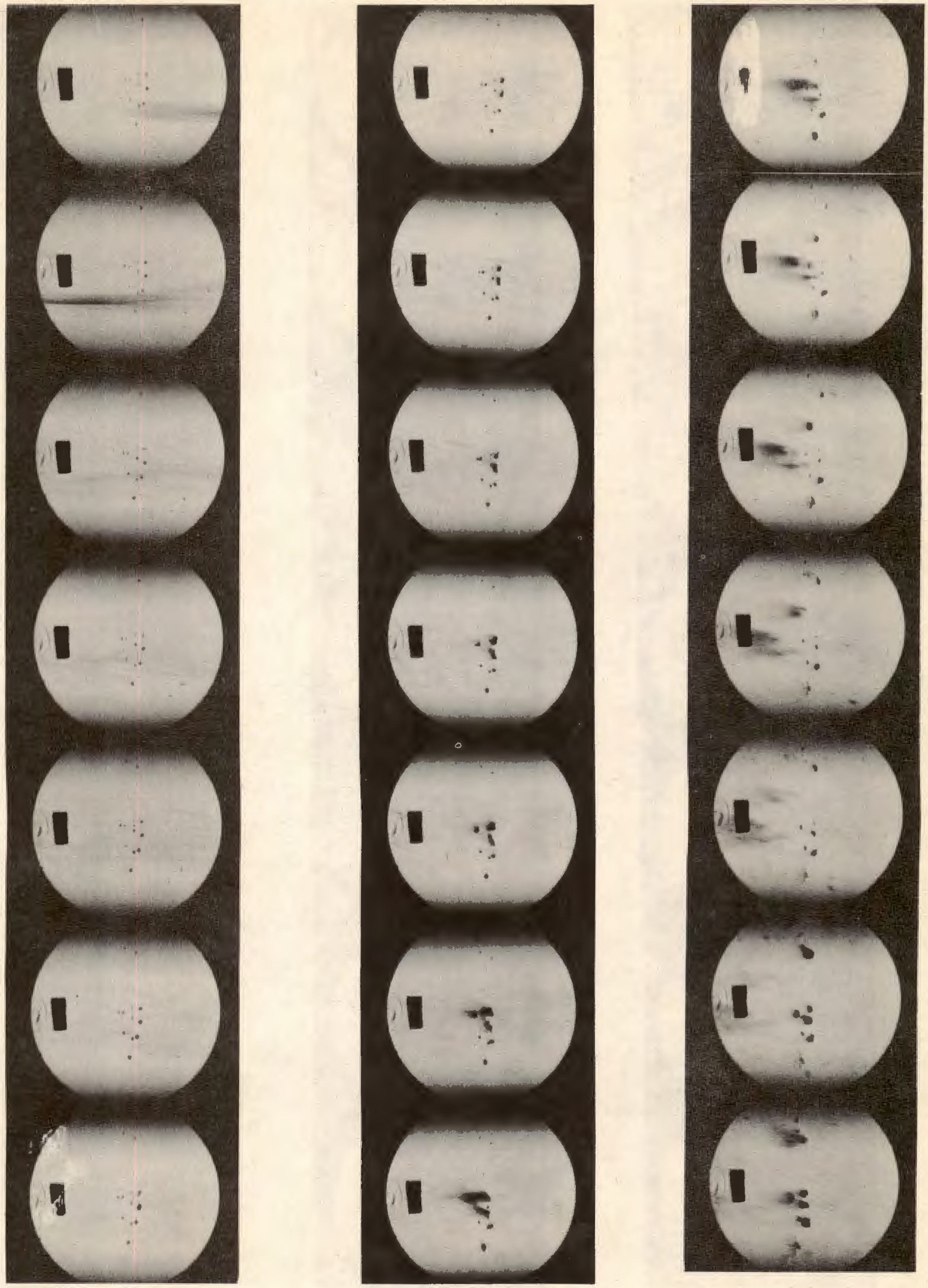

Shot No. 1. Conical-Nose Projectile 60-Caliber with 60° Full Apex Angle
Speed 4060 ft/sec

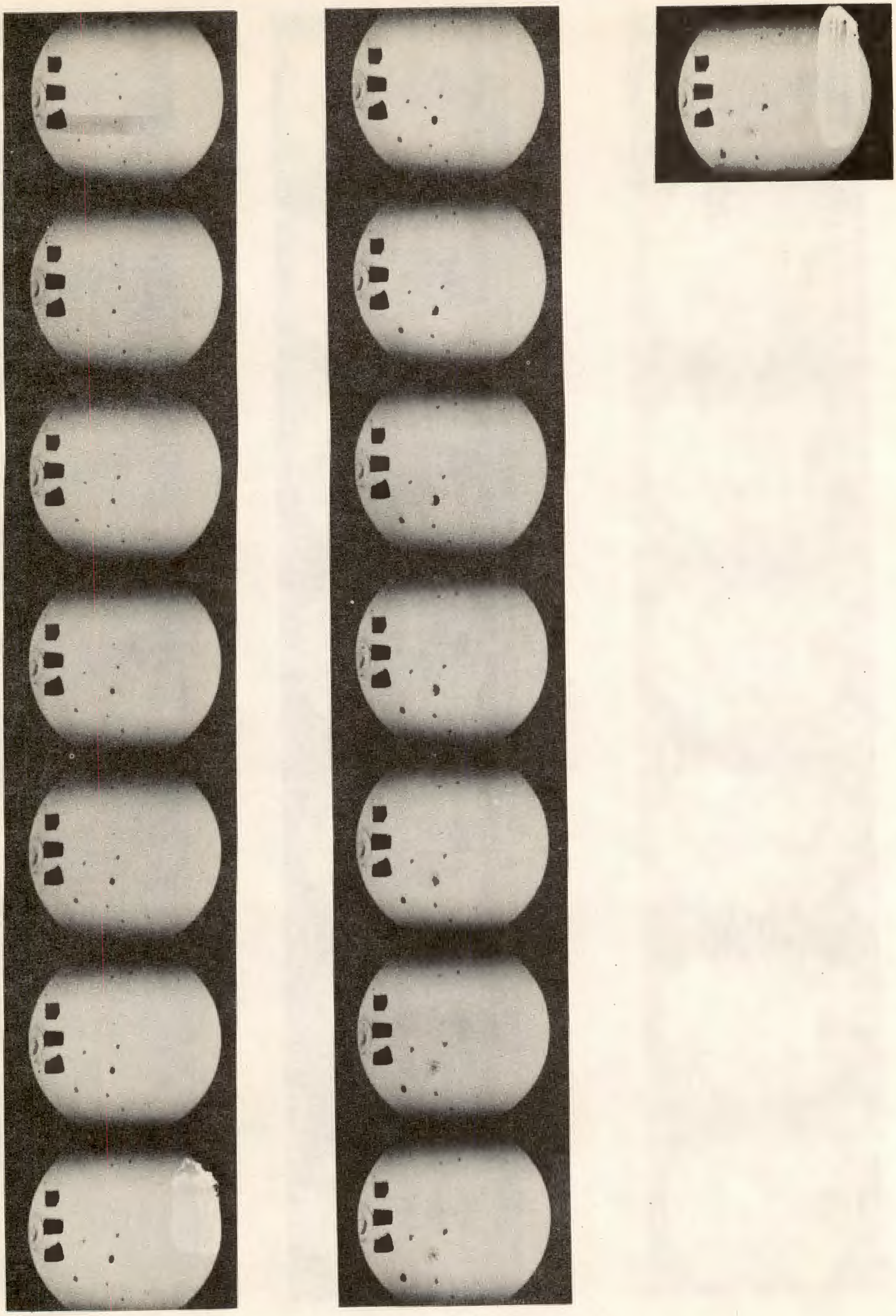

Shot No. 3. Conical-Nose Projectile 60-Caliber with 60° Full Apex Angle
Speed 3140 ft/sec

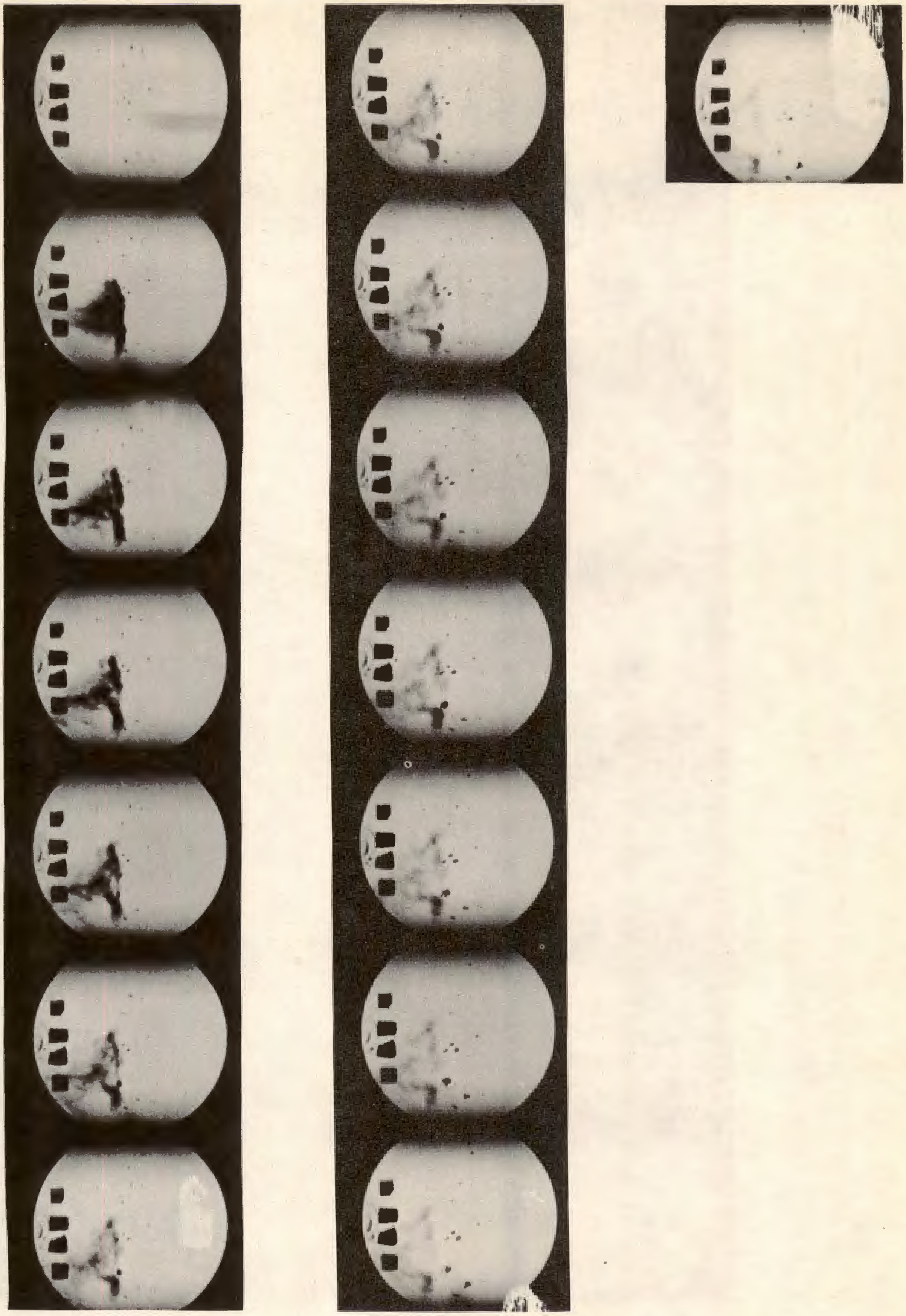

Shot No. 4. Conical-Nose Projectile 60-Caliber with 60° Full Apex Angle
Speed 2910 ft/sec

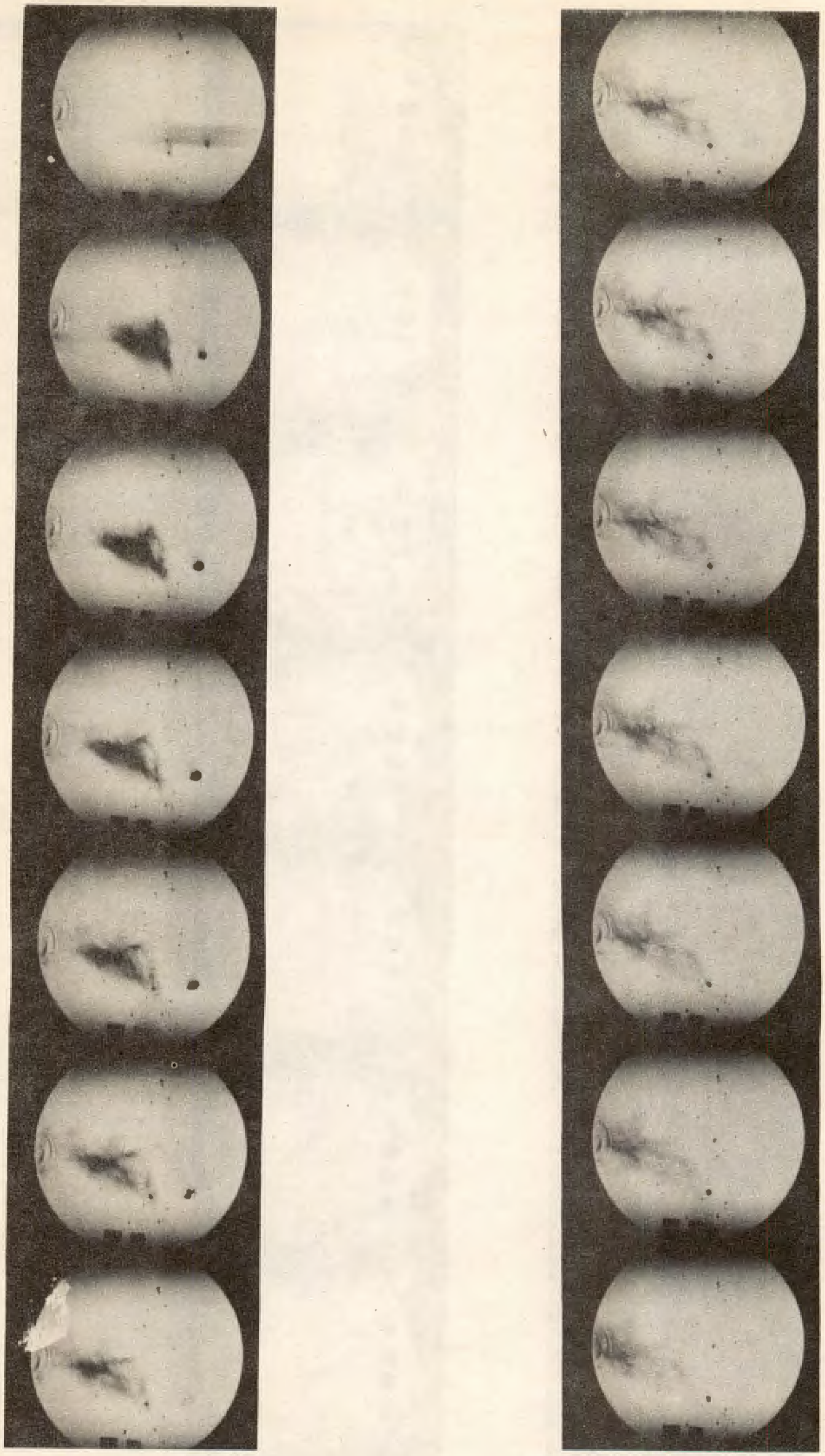

Shot No. 6. Conical-Nose Projectile 60-Caliber with 60° Full Apex Angle
Speed 2730 ft/sec

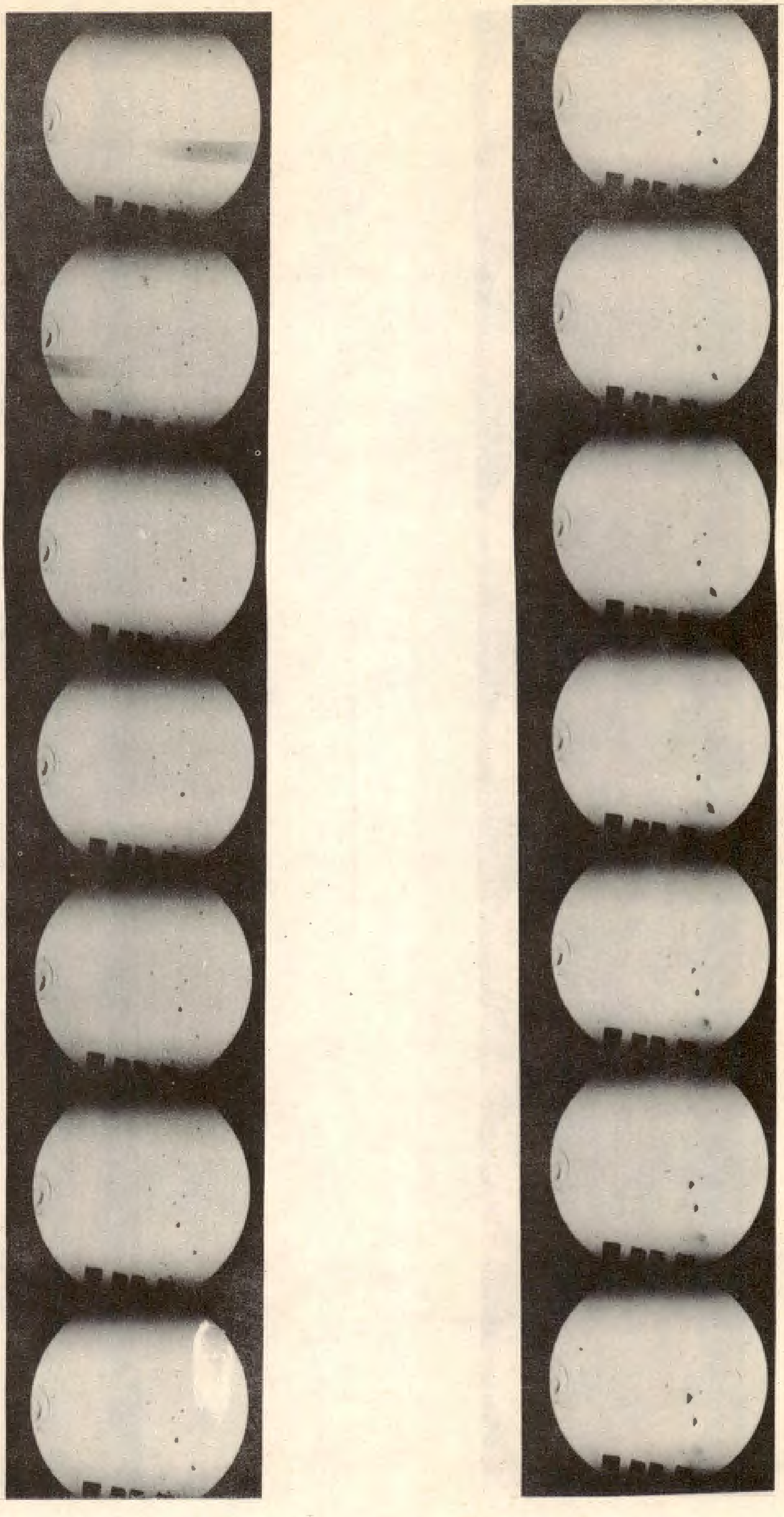

Shot No. 8. Conical-Nose Projectile 60-Caliber with 60° Full Apex Angle
Speed 2510 ft/sec

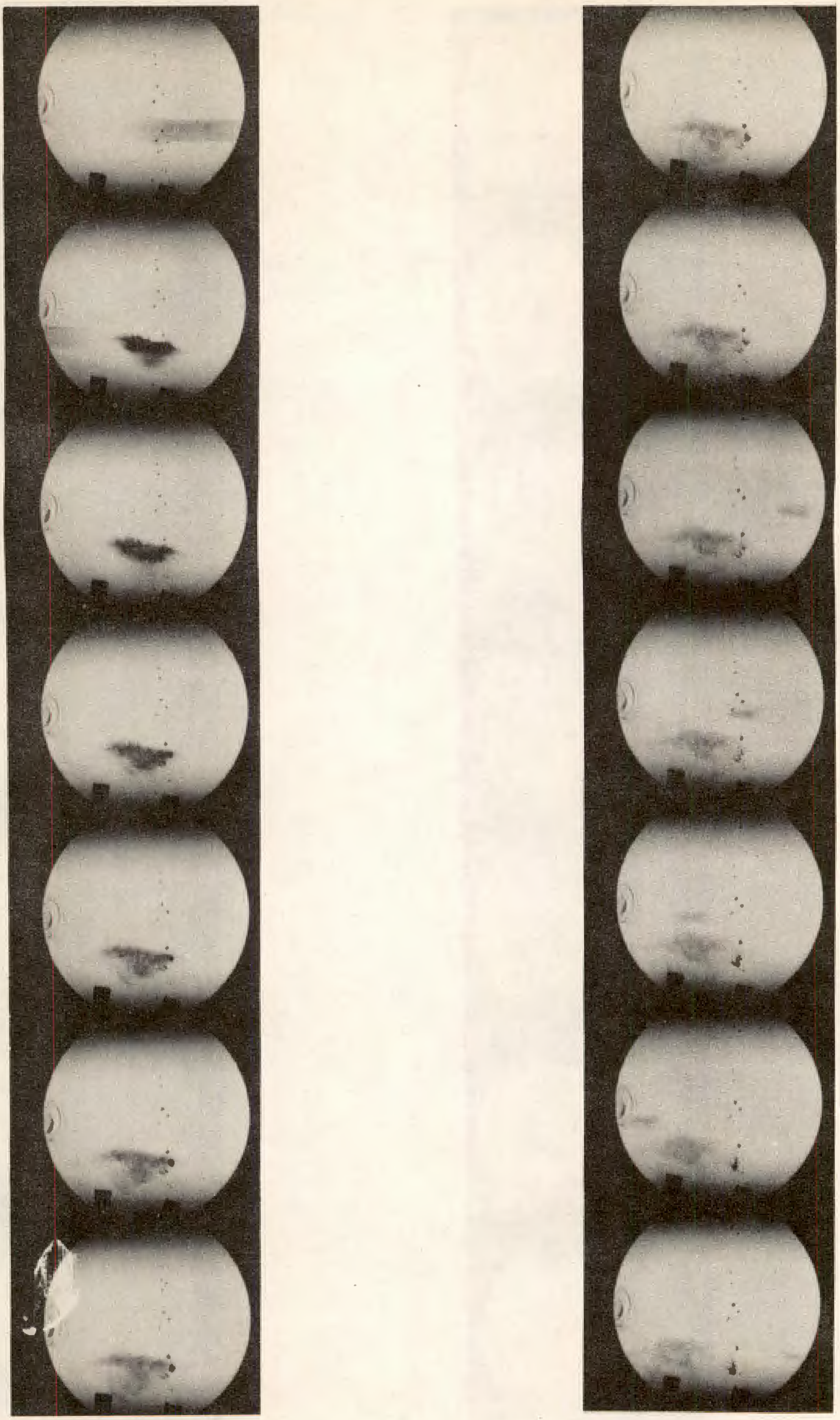

Shot No. 10. Conical-Nose Projectile 60-Caliber with 60° Full Apex Angle
Speed 2680 ft/sec

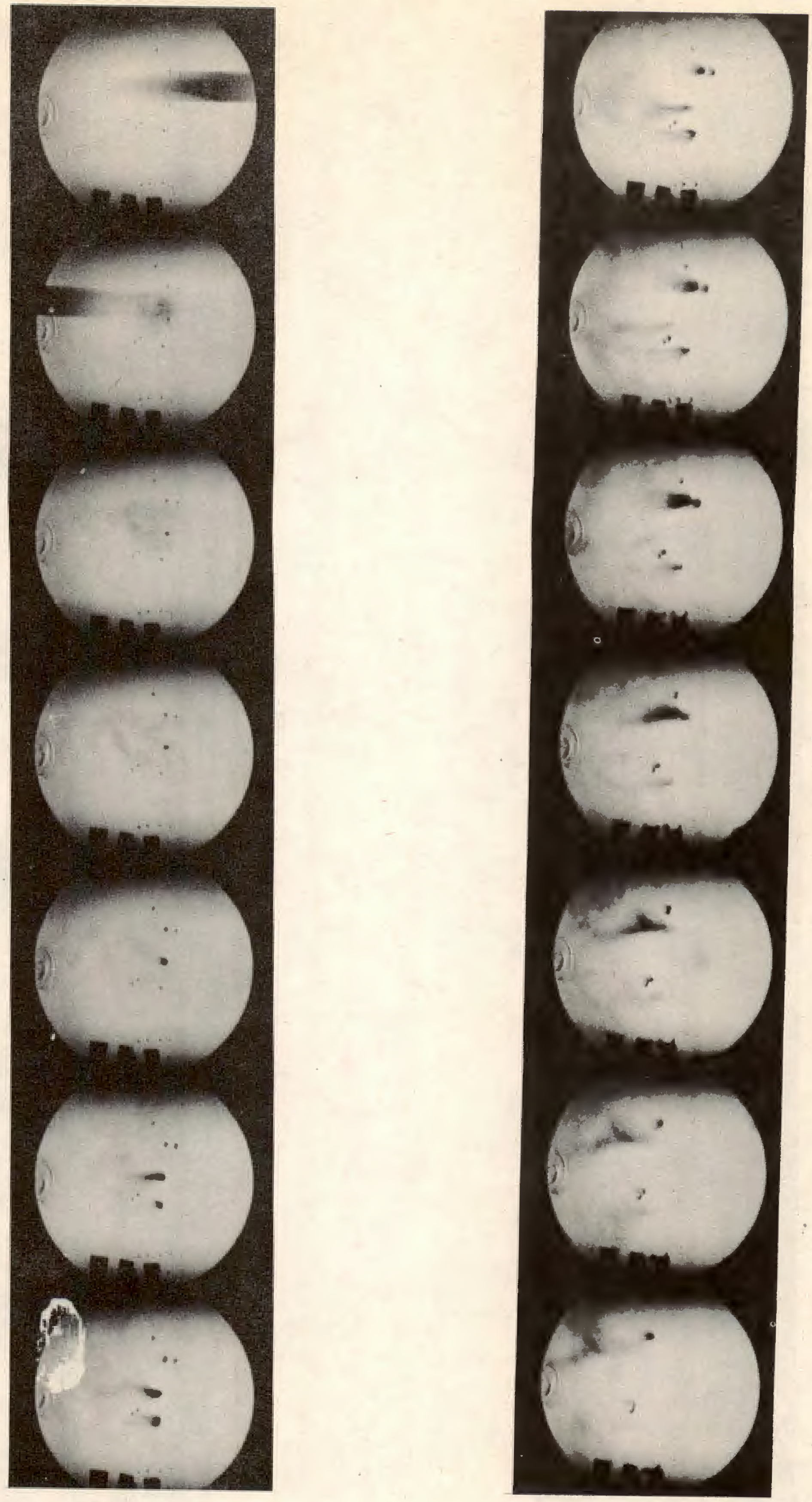

Shot No. 14. 20-mm Projectile, Speed 2660 ft/sec

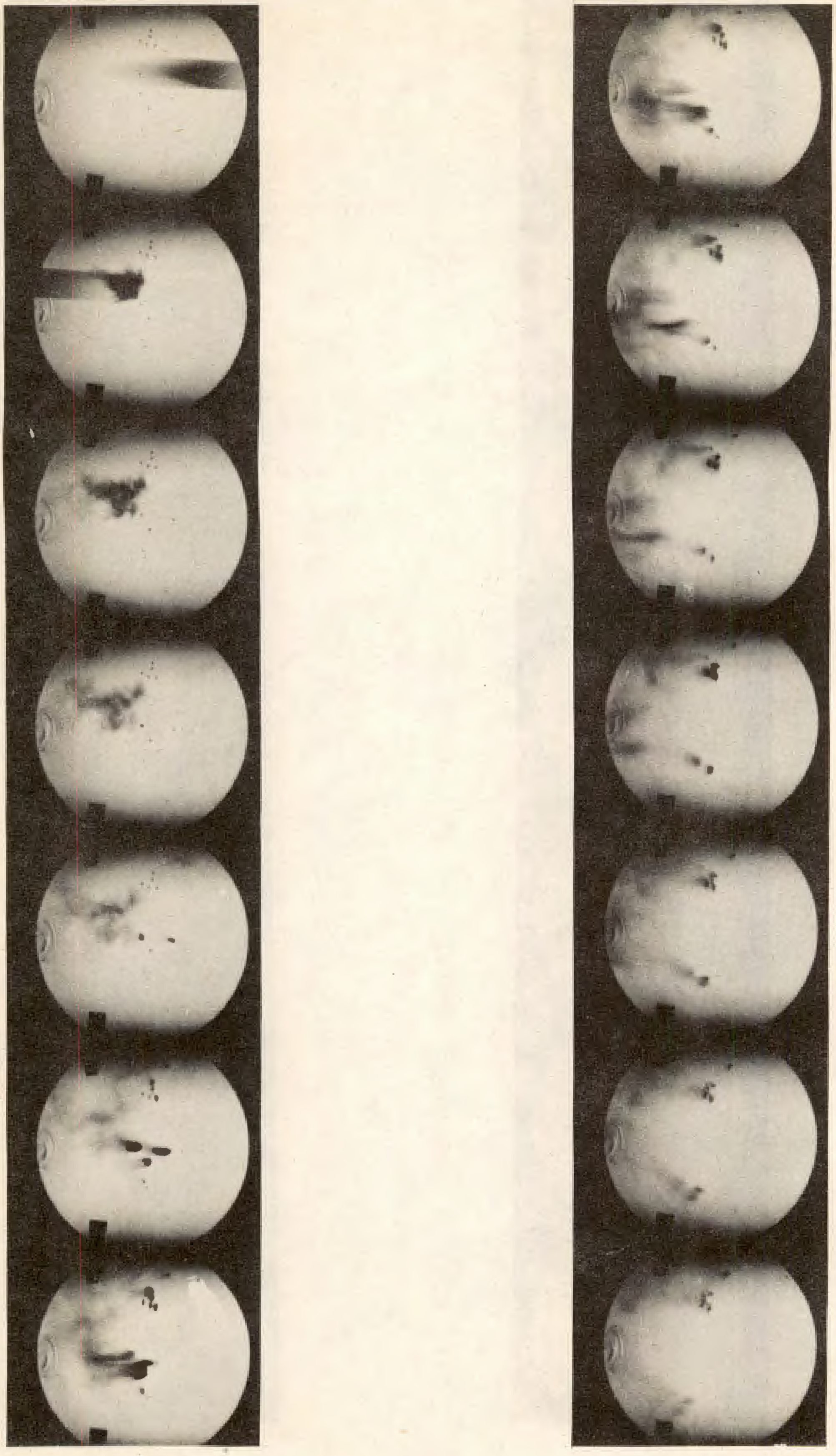

Shot No. 15. 20-mm Projectile, Speed 2720 ft/sec
Vol. I

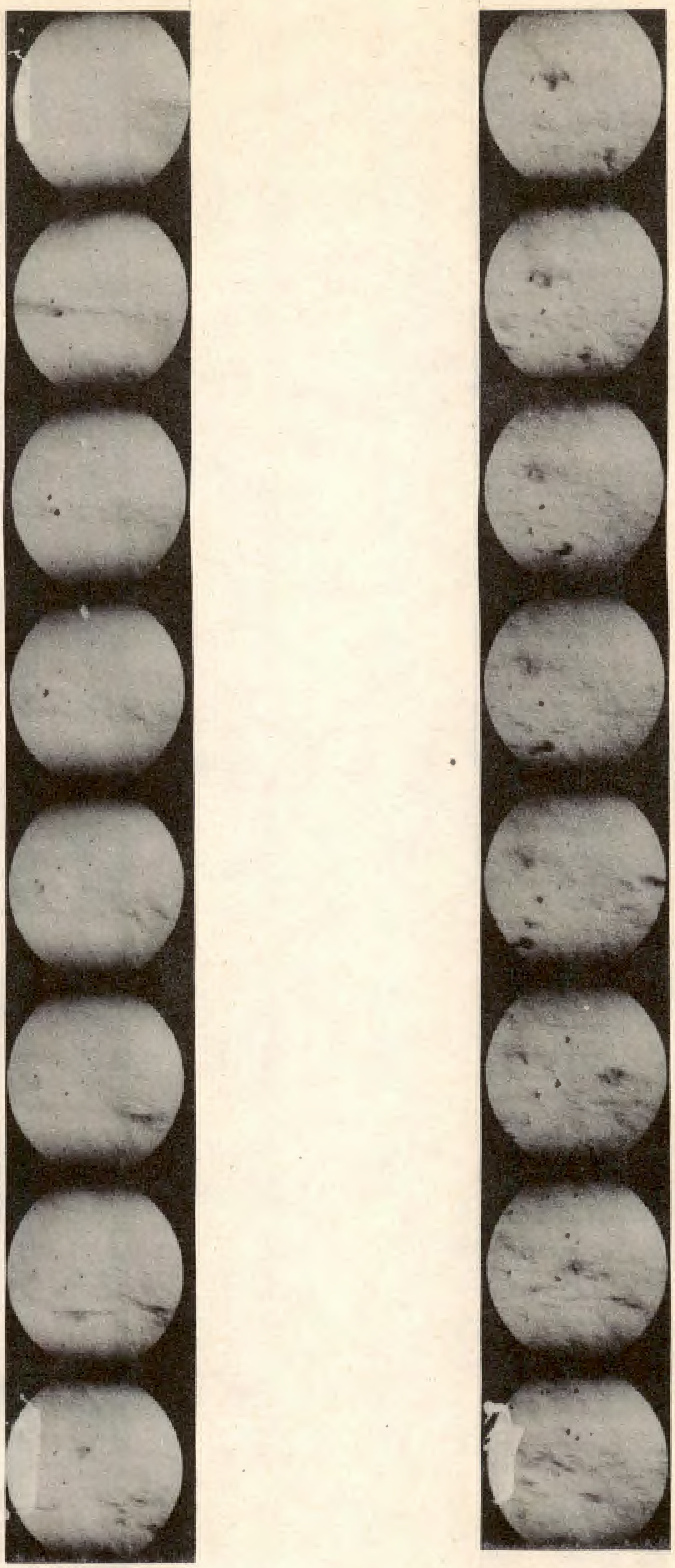

Shot No. 19. Bluff-Nose Cylindrical 60-Caliber, Speed 1900 ± 100 ft/sec

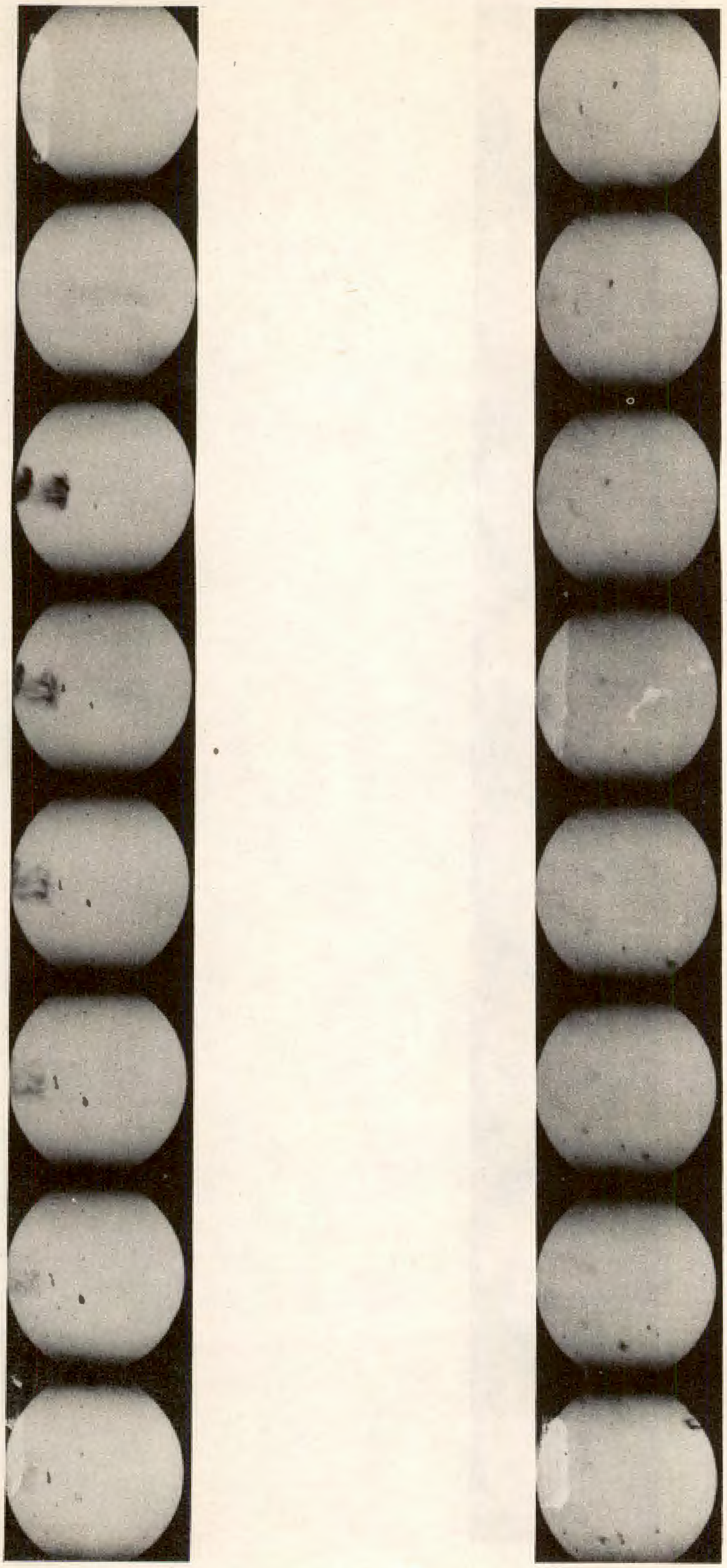

Shot No. 20. Bluff-Nose Cylindrical 60-Caliber, Speed 1900 ± 100 ft/sec

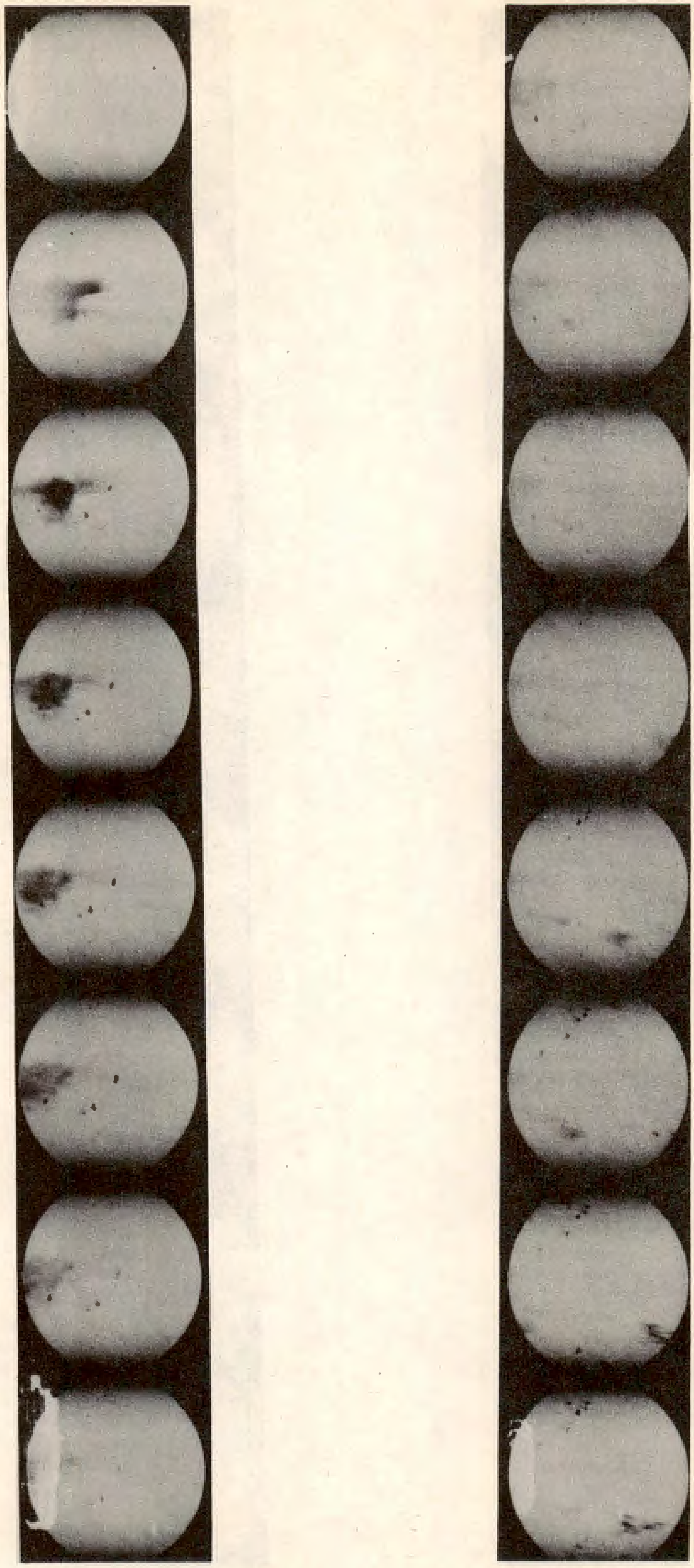

Shot No. 21. Bluff-Nose Cylindrical 60-Caliber, Speed 1900 ± 100 ft/sec

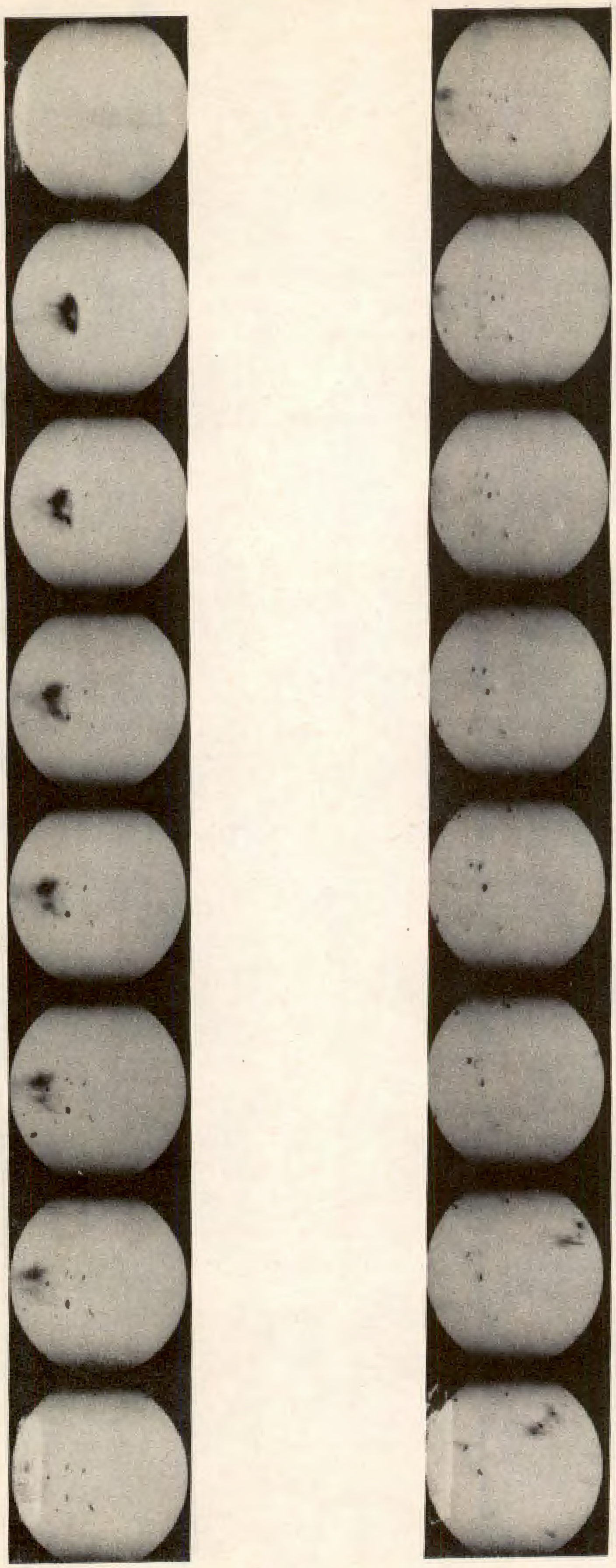

Shot No. 22. Bluff-Nose Cylindrical 60-Caliber. Speed 1900 ± 100 ft/sec